Supporting Information

Uncovering the Encapsulation Effect of Reduced Graphene Oxide Sheets on Hydrogen Storage Properties of Palladium Nanocubes

Jinseok Koh,[a] Eunho Choi,[b] Kouji Sakaki,[c] Daeho Kim,[d] Seung Min Han,[d] Sangtae Kim,*[b] and Eun Seon Cho*[a]

[a] *Department of Chemical and Biomolecular Engineering, Korea Advanced Institute of Science and Technology (KAIST), Daejeon 34141, Republic of Korea*

[b] *Department of Nuclear Engineering, Hanyang University, Seoul 04763, Republic of Korea*

[c] *Energy Process Research Institute, National Institute of Advanced Industrial Science and Technology (AIST), 16-1 Onogawa, Tsukuba, Ibaraki 305-8569, Japan*

[d] *Department of Materials Science and Engineering, Korea Advanced Institute of Science and Technology (KAIST), Daejeon 34141, Republic of Korea*

Corresponding Authors

*Email: sangtae@hanyang.ac.kr (S. Kim)

*Email: escho@kaist.ac.kr (E. S. Cho)

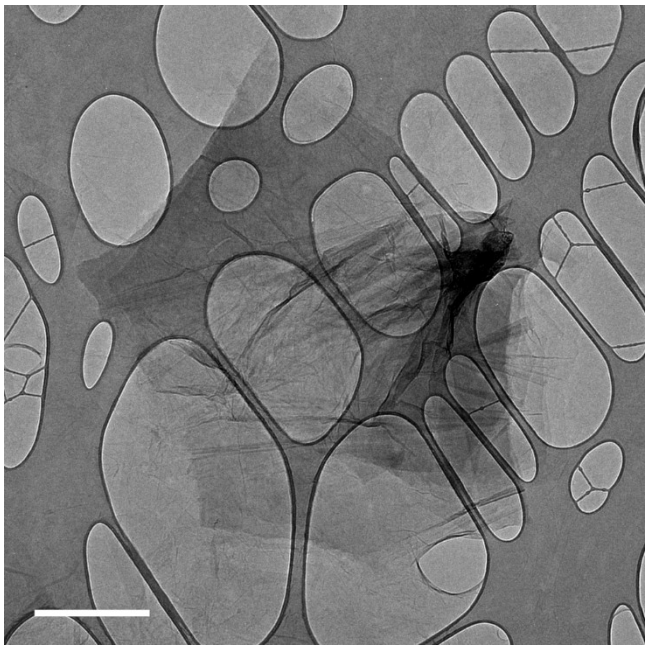

Fig. S1 TEM image of the neat GO sheets which are well exfoliated (the scale bar is 1μm).

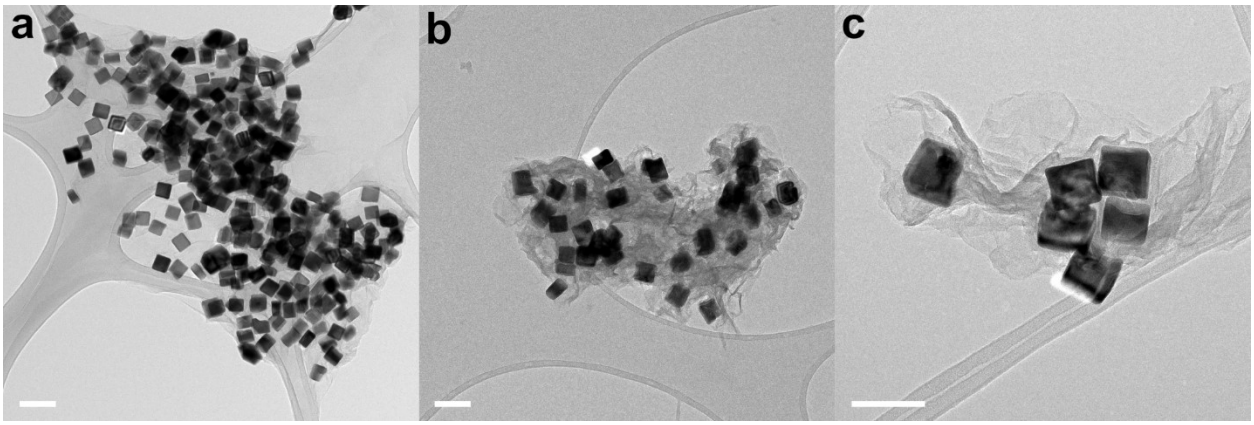

Fig. S2 Low magnified TEM images of (a) rGO-Pd1, (b) rGO-Pd2, and (c) rGO-Pd3 (the scale bar is 100 nm).

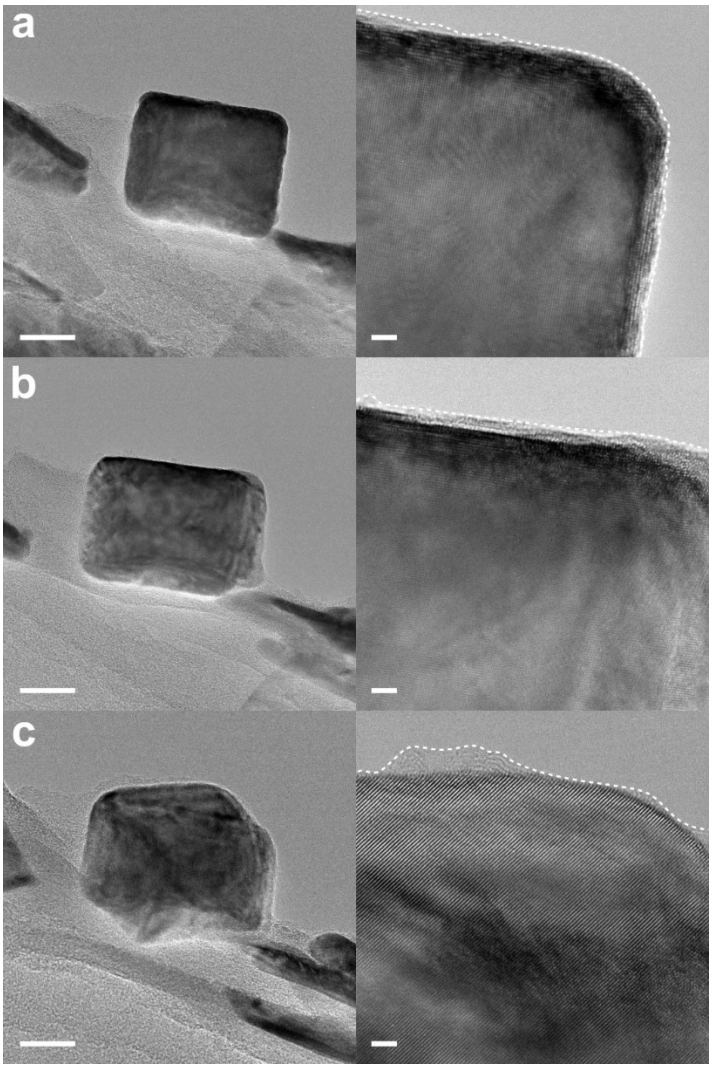

Fig. S3 HRTEM images of rGO-Pd2 oriented along the (a) [001], (b) [013], and (c) [112] zone axis (the scale bars indicate 20 nm). The right panels show the magnified views of the corresponding Pd nanocube (the scale bars represent 2 nm). White dashed lines represent the outermost rGO layers.

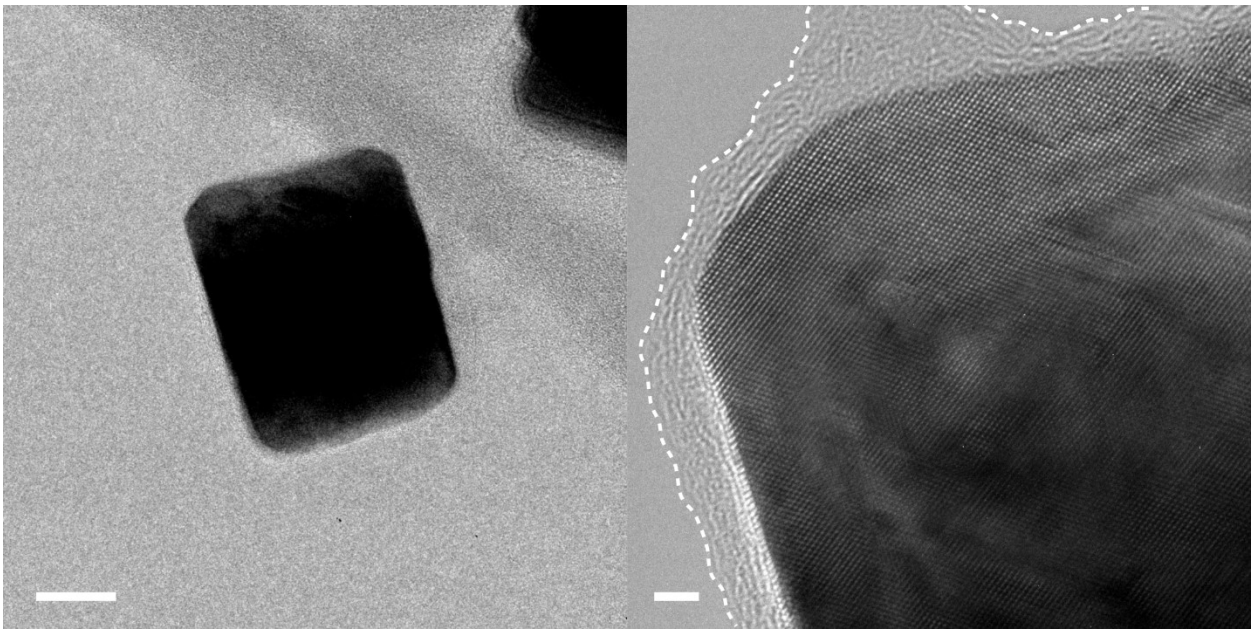

Fig. S4 (Left) HRTEM image of the [110] zone axis oriented Pd nanocube from another rGO-Pd2 sample (the scale bar is 20 nm). (Right) The magnified view of the Pd nanocube shows the layered-encapsulating structure (the scale bar is 2 nm).

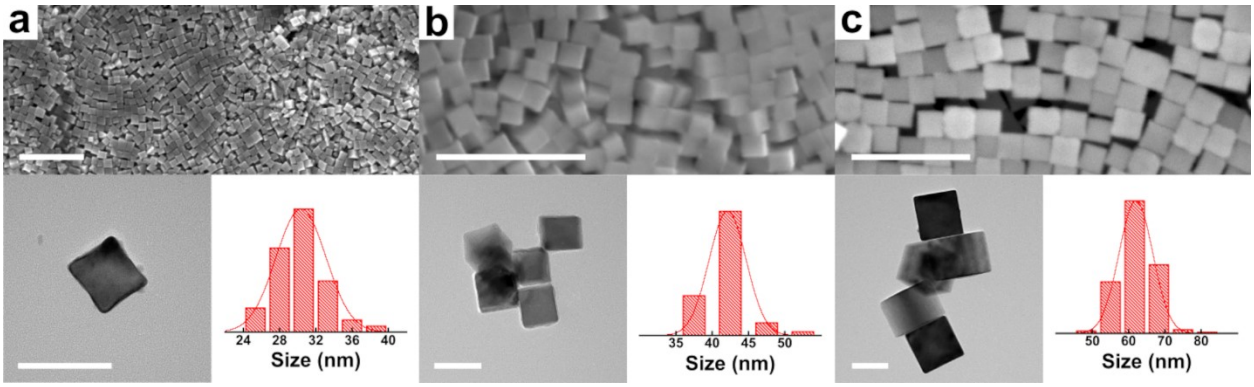

Fig. S5. SEM (upper panel; the scale bars represent 300 nm) and TEM (lower panel; the scale bars indicate 50 nm) images of bare-Pd nanocubes with an edge size of (a) 30.4 ± 2.8 nm, (b) 42.1 ± 2.6 nm, and (c) 62.0 ± 4.6 nm with their size distributions.

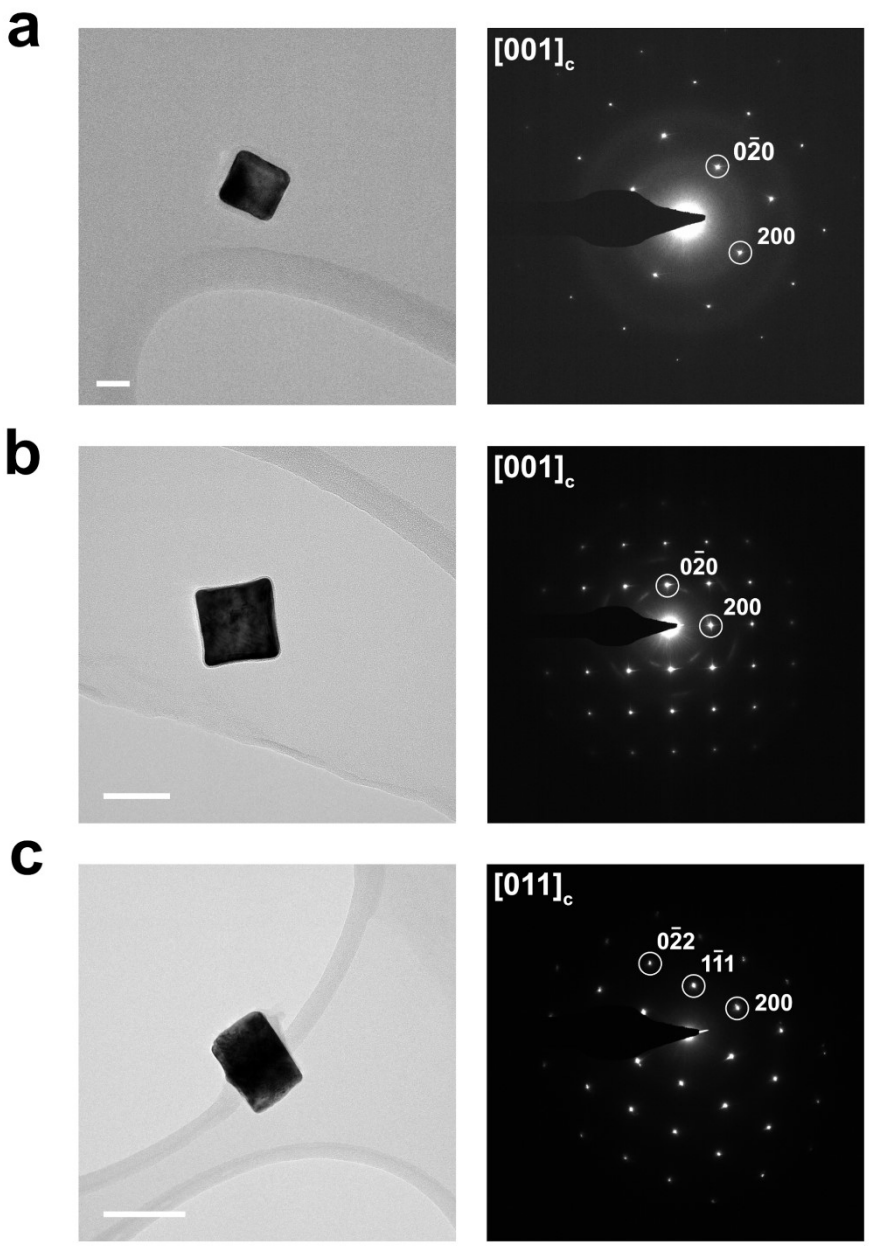

Fig. S6 TEM images (left) and the corresponding SAED patterns (right) of (a) rGO-Pd1, (b) rGO-Pd2, and (c) rGO-Pd3 (the scale bars indicate 20 nm, 50 nm, and 100 nm, respectively).

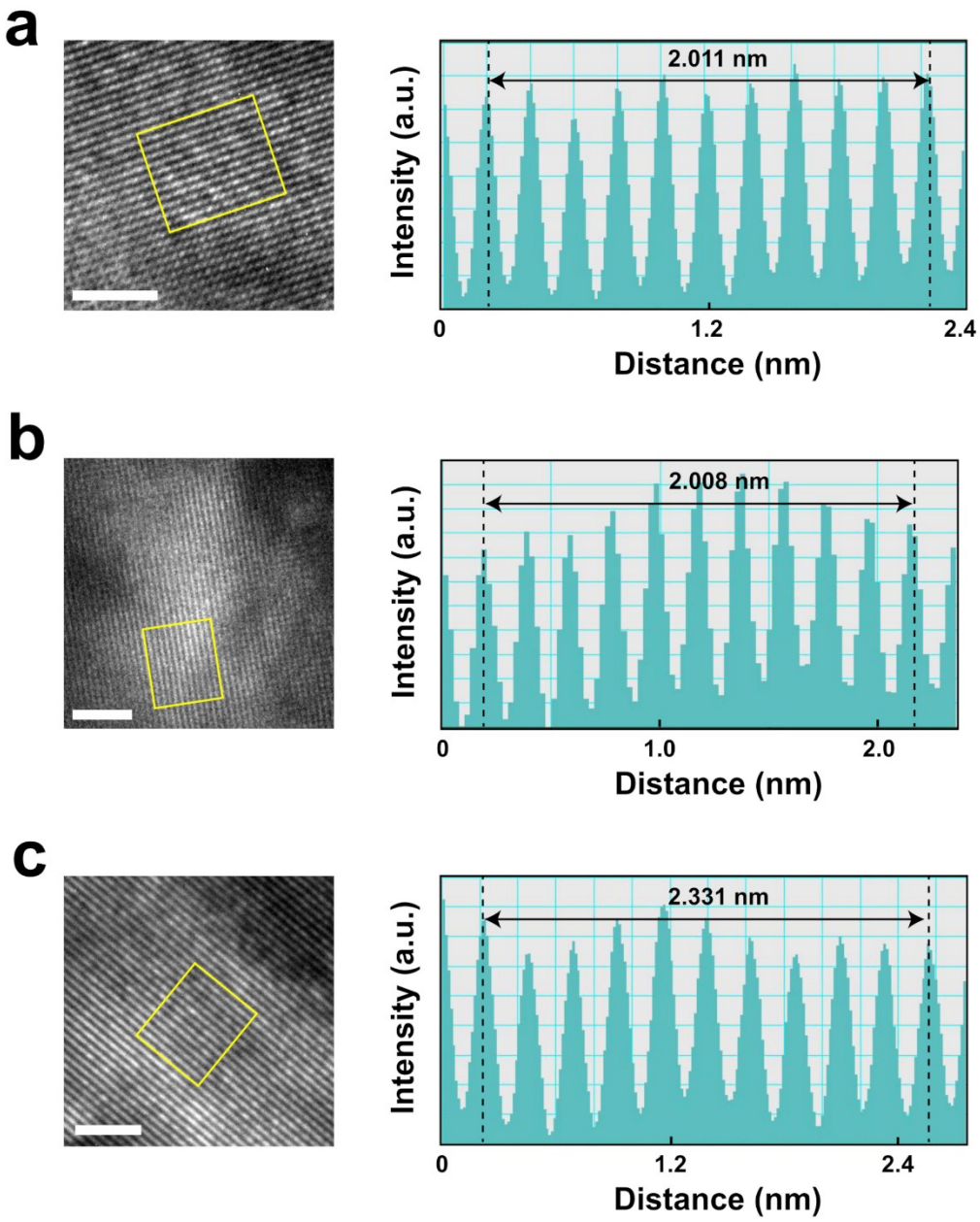

Fig. S7 HRTEM images (left) and the corresponding lattice spacing intensity profiles (right) of (a) rGO-Pd1, (b) rGO-Pd2, and (c) rGO-Pd3 (all scale bars indicate 2 nm).

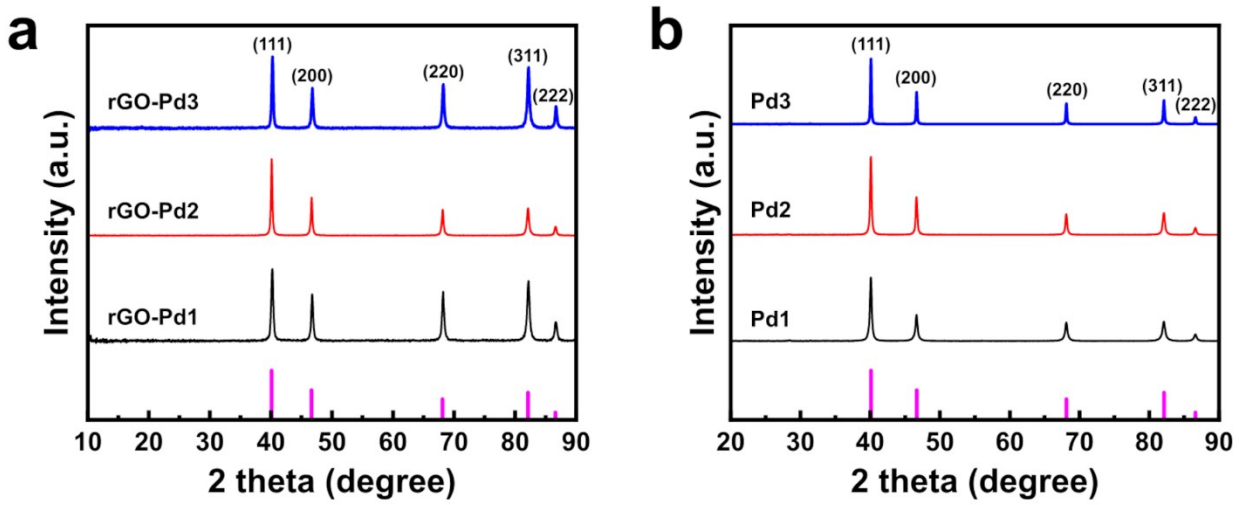

Fig. S8 XRD patterns of (a) rGO-Pd and (b) bare-Pd nanocubes; the bottom bars show peak positions of XRD pattern of bulk Pd with FCC structure (PDF # 00-046-1043).

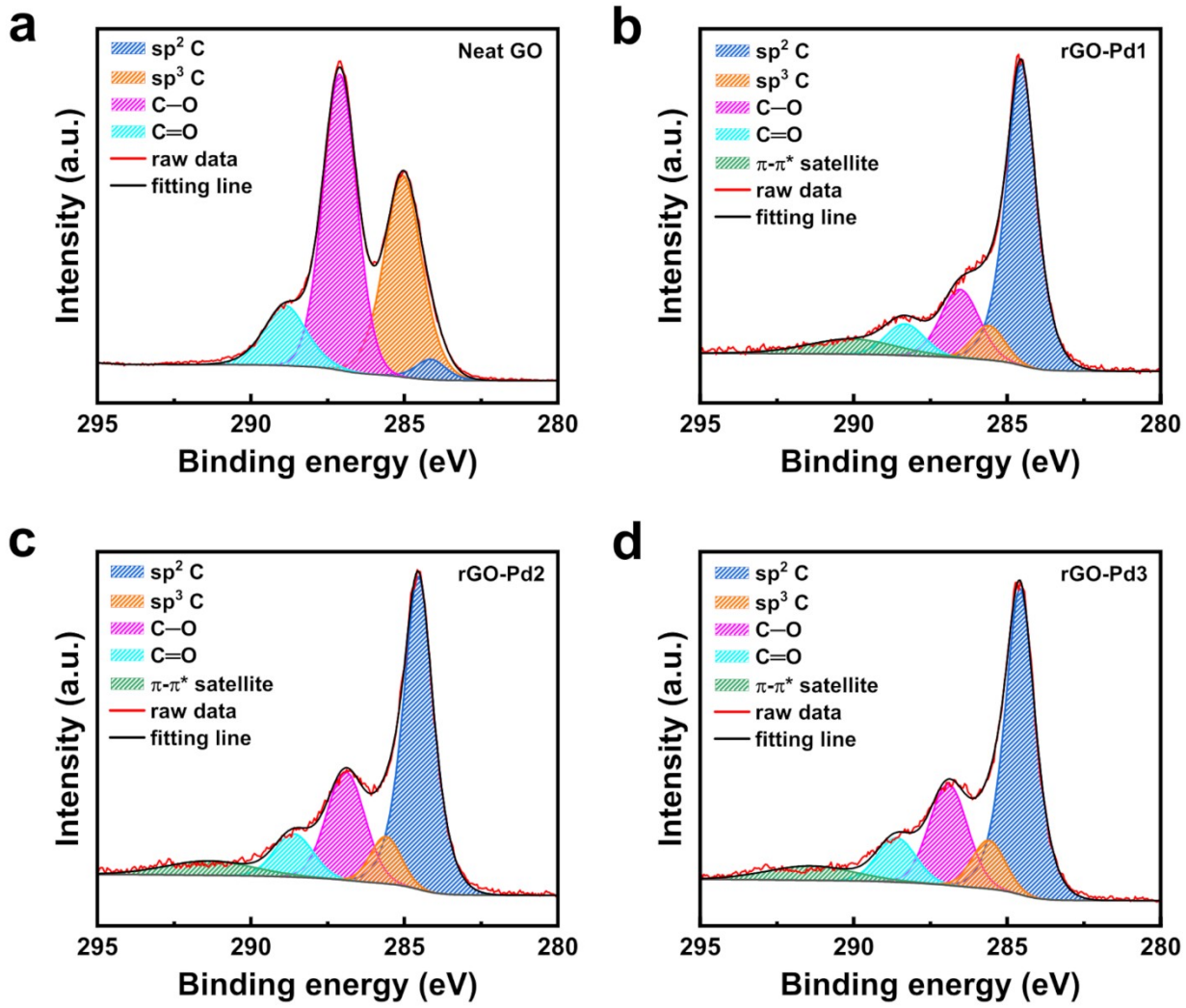

Fig. S9 C 1s XPS spectra from (a) neat GO and (b-d) rGO-Pd nanocubes.

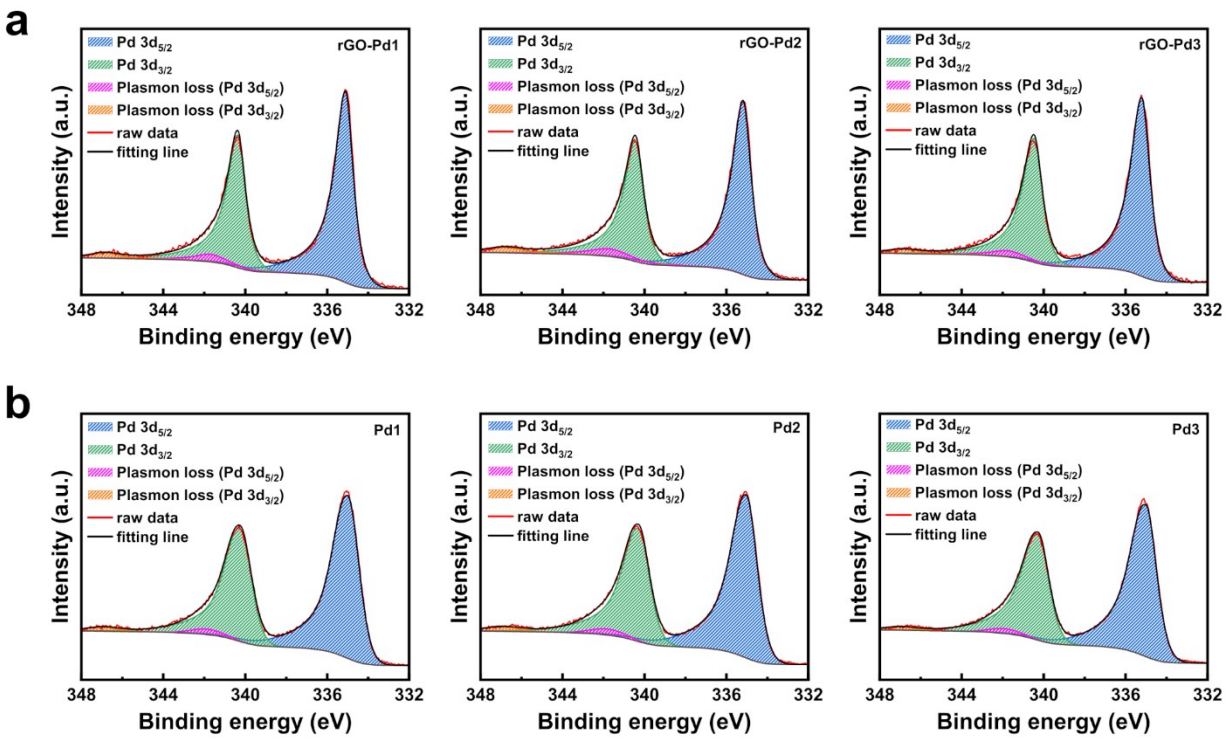

Fig. S10 Pd 3d XPS spectra from (a) rGO-Pd and (b) bare-Pd nanocubes. The binding energies of both Pd $3d_{5/2}$ and Pd $3d_{3/2}$ peaks are barely changed within 0.2 eV, indicating a weak electron transfer.

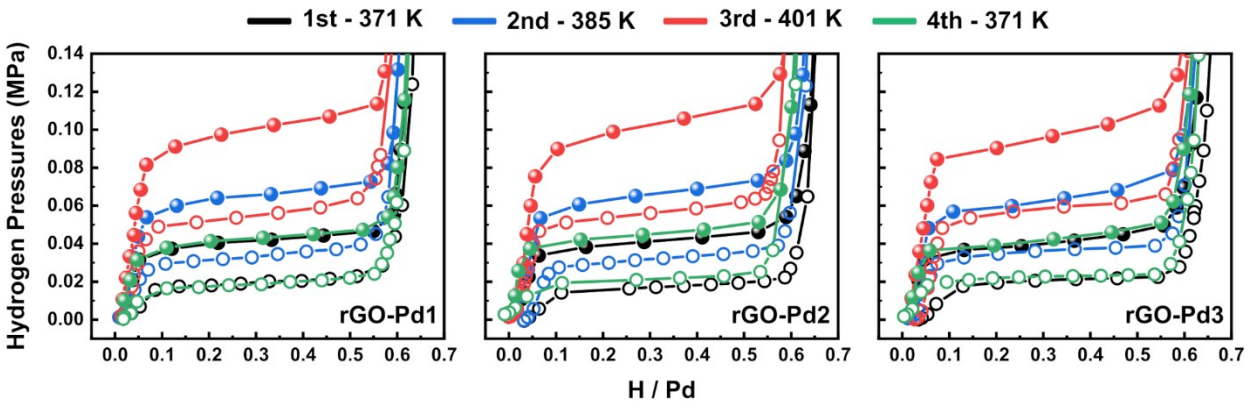

Fig. S11 PC isotherms of rGO-Pd samples during multiple hydrogen sorption cycles at 371 K, 385 K, and 401 K. Repeated experiments even after the high temperature cycle (3rd-401 K) show nearly identical de/hydriding profiles (1st-371K and 4th-371K).

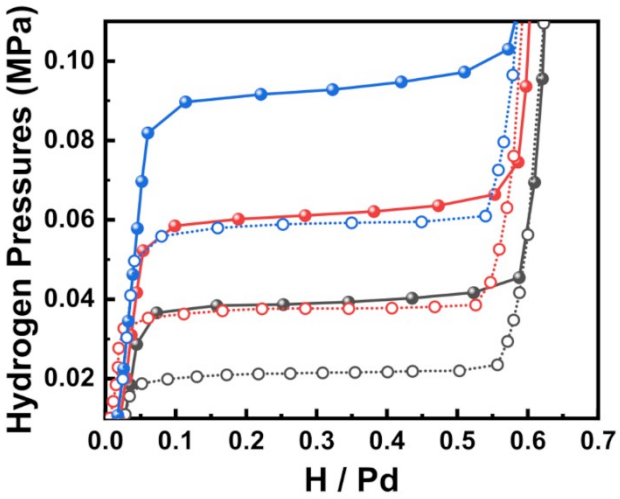

Fig. S12 PC isotherms of bulk Pd at 371 K (black line), 385 K (red line), and 401 K (blue line) during absorption (solid circle) and desorption (open circle) process.

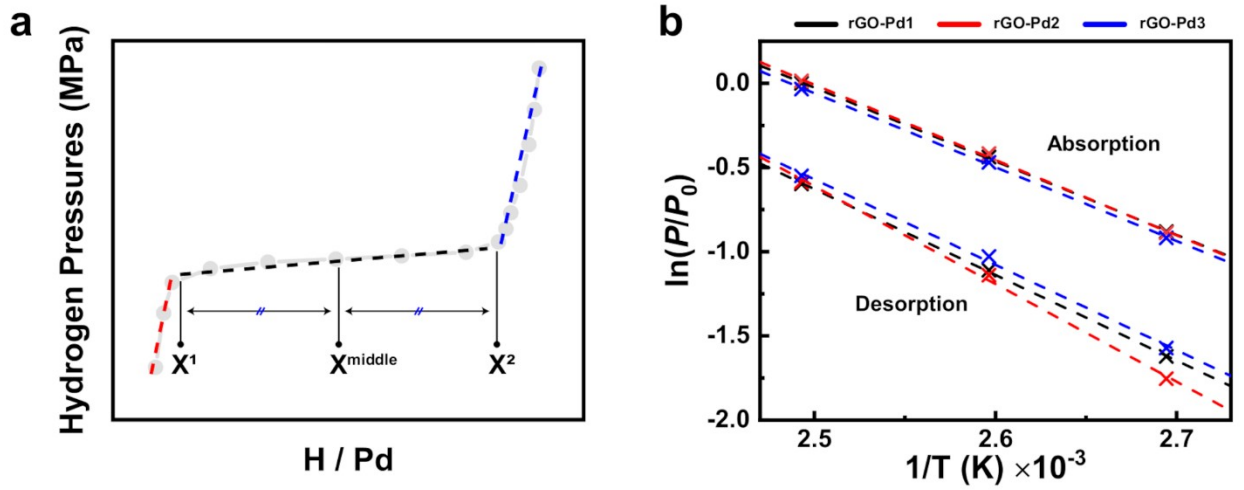

Fig. S13 (a) Abbreviated PC isotherms which schematically present the procedure for determining the plateau pressure. The isotherm can be divided into three regions: solid solution (α–phase), transition region, hydrogen-rich region (β–phase). We fitted each region using linear regression and found the intersection points of adjacent phases (X^1 and X^2). With the middle of two points (X^{middle}), the plateau pressure was obtained. (b) The van't Hoff plots fitted from isotherm data of rGO-Pd.

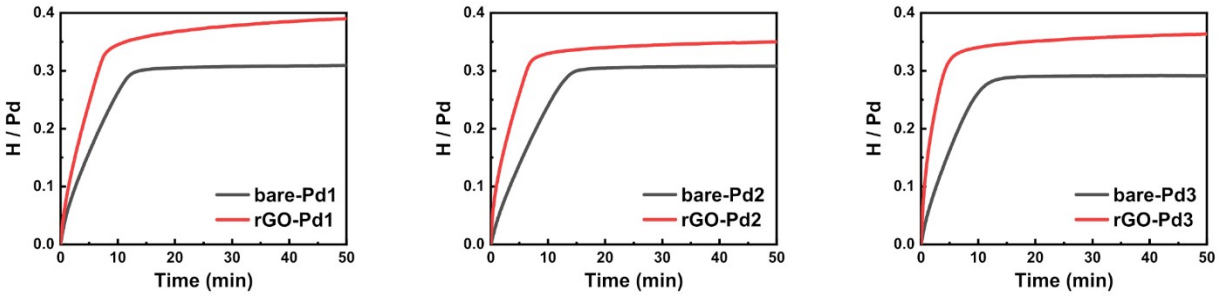

Fig. S14 Hydrogen absorption at 303 K under 1.3 bar of H_2 pressure for rGO-Pd and bare-Pd nanocubes.

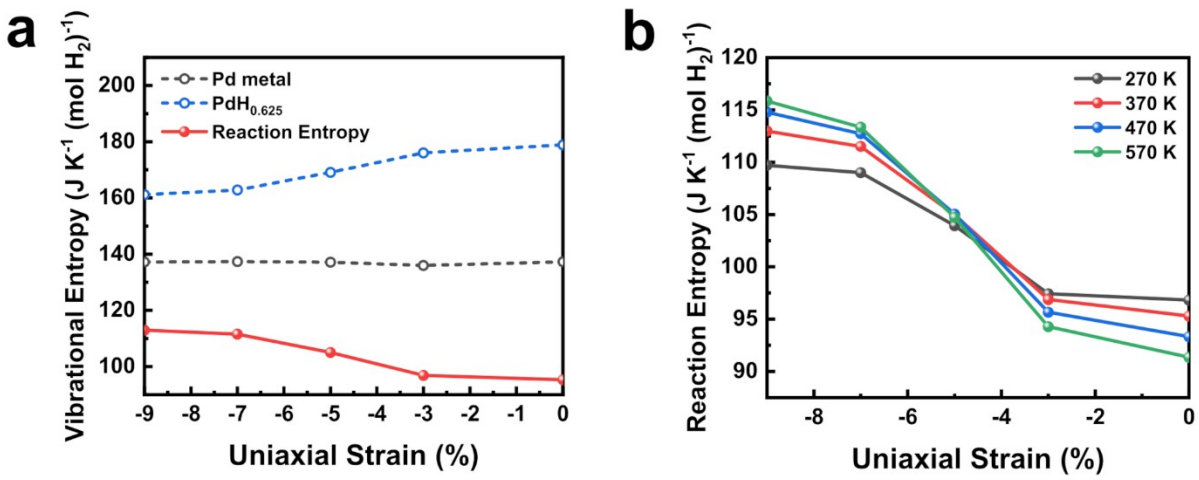

Fig. S15 (a) Computed reaction entropy and vibrational entropy of $PdH_{0.625}$ and Pd at the varied uniaxial compression from 0 to 9 %, while allowing Poisson expansion. (b) Desorption entropy computed at varied temperatures between 270 K and 570 K under uniaxial compression.